

Exploring the behavior of electron-hole pairs in working organic light emitting diodes

Shuto Hatanaka, Keigo Kimura, Takayuki Suzuki,
Katsuichi Kanemoto

Citation	Physical Review Materials, 2(11); 115201
Issue Date	2018-11-08
Type	Journal Article
Textversion	publisher
Rights	©American Physical Society. This article may be downloaded for personal use only. Any other use requires prior permission of the author and American Physical Society. The following article appeared in Physical Review Materials Vol.2, Iss.11 and may be found at https://doi.org/10.1103/PhysRevMaterials.2.115201
DOI	10.1103/PhysRevMaterials.2.115201

Self-Archiving by Author(s)
Placed on: Osaka City University

Exploring the behavior of electron-hole pairs in working organic light emitting diodes

Shuto Hatanaka,¹ Keigo Kimura,¹ Takayuki Suzuki,² and Katsuichi Kanemoto^{1,*}¹*Department of Physics, Graduate School of Science, Osaka City University, 3-3-138 Sugimoto, Sumiyoshi-ku, Osaka 558-8585, Japan*²*JEOL RESONANCE Inc., 3-1-2 Musashino, Akishima, Tokyo 196-8558, Japan*

(Received 19 July 2018; published 8 November 2018)

Although the conversion reactions of electron-hole (e-h) pairs into emissive excitons are essential in the operation process of organic light emitting diodes (OLEDs), experimental research on behaviors of e-h pairs in operating OLEDs has not been developed so far. Here, three types of magnetic-resonance techniques that detect changes in current, photoluminescence intensity, and electroluminescence (EL) intensity induced by electron spin-resonance transitions have been applied to a working OLED as a function of operation bias. Combined use of these techniques reveals that e-h pairs exist in the OLED with completely different bias dependence from carriers and excitons. It is shown that the EL process is classified into three regions depending on the bias: pair-accumulation, pair-dissociation/recombination, and non-pair-formation regions.

DOI: [10.1103/PhysRevMaterials.2.115201](https://doi.org/10.1103/PhysRevMaterials.2.115201)

Since the first discovery of prominent electroluminescence (EL) effect from organic materials [1,2], organic light emitting diodes (OLEDs) have undergone much technological progress via intensive research from academia and industry and recently reached a commercial stage enabling even applications to portable displays. The progress was made by designing efficient OLEDs such as phosphorescent OLEDs with a high photon generation ratio [3–5] and fluorescent OLEDs utilizing thermally activated delayed fluorescence from triplet excitons (TEs) to singlet excitons (SEs) [6–8]. Despite such progress, the reaction process of the excitons has not been sufficiently explored. It is because effective experimental techniques to extract information from the reaction have not been developed. Developing such experimental techniques must be effective for improving the OLED performance in common with all types of OLEDs.

It is generally explained that an EL process occurs via recombination of holes and electrons injected from electrodes to generate SEs and TEs and the main emission is given by either exciton. However, indeed, in the EL process, electron-hole (e-h) pairs (or polaron pairs) consisting of weakly coupled electron and hole are expected to exist as intermediate states between the carriers and excitons. The weak coupling should be sensitive to electric field and thus the e-h pairs could affect largely the bias dependence of the OLED process. Moreover, the e-h pairs have also been regarded as one of the elements to induce magnetic-field effects in the EL-intensity and -conductivity of OLEDs [9–16]. Revealing the behavior of the e-h pair is thus significant not only for investigating the OLED operation process but also for considering magnetic properties of OLED. Nonetheless, since such temporal intermediate species are experimentally difficult to examine, the behavior of the e-h pairs in operating LEDs has not been sufficiently explored.

For considering the properties of e-h pairs, we focus on an equilibrium relation formed among carriers, e-h pairs, and excitons in operating OLEDs [Fig. 1(a)]. An ESR transition occurring at sublevels of triplet e-h pair (TP) slightly changes the density ratio between singlet e-h pair (SP) and TP through spin mixing of S and T_0 . The change of the pair density leads to changing the densities of carriers and luminescent excitons, which can be observed from current and luminescence measurements synchronized with the ESR transition, termed generally electrically detected and optically detected magnetic resonance (EDMR and ODMR) measurements, respectively. Recently, in fact, the properties of photogenerated e-h pairs were investigated from EDMR and ODMR under photoexcitation (photocurrent DMR and photoluminescence (PL) DMR, respectively). From the bias dependence of their signal intensities, the e-h pairs were suggested to be dissociated by the electric field from the applied bias [17]. The results were obtained under reverse bias where carrier injection from the electrodes is negligible. By contrast, under forward bias where EL occurs, it is predicted that not only the dissociation of e-h pairs but also the generation of e-h pairs occurs depending on the bias, making bias-dependent behaviors of e-h pair complicated. Thus, in order to clarify the behavior of e-h pairs under OLED operation, such coexisting bias-dependent processes must be experimentally classified for evaluation.

In this paper, the bias-dependent behaviors of e-h pairs in working OLEDs are investigated from the EDMR technique for the dark current and an EL-detected magnetic resonance (ELDMR) technique for a basic OLED with a single active layer. For these techniques, the condition of driving OLED is changed by controlling the operation bias and their ESR responses involved are tracked. In addition to these ESR techniques, a PLDMR technique under the forward bias is also applied to the OLED. The use of these ESR techniques as a function of bias enables experimental discrimination of bias-dependent multiple processes in e-h pairs. It is revealed that the e-h pairs are not simply generated linearly for the increase of carriers and excitons. The EL process is found to

*kkane@sci.osaka-cu.ac.jp

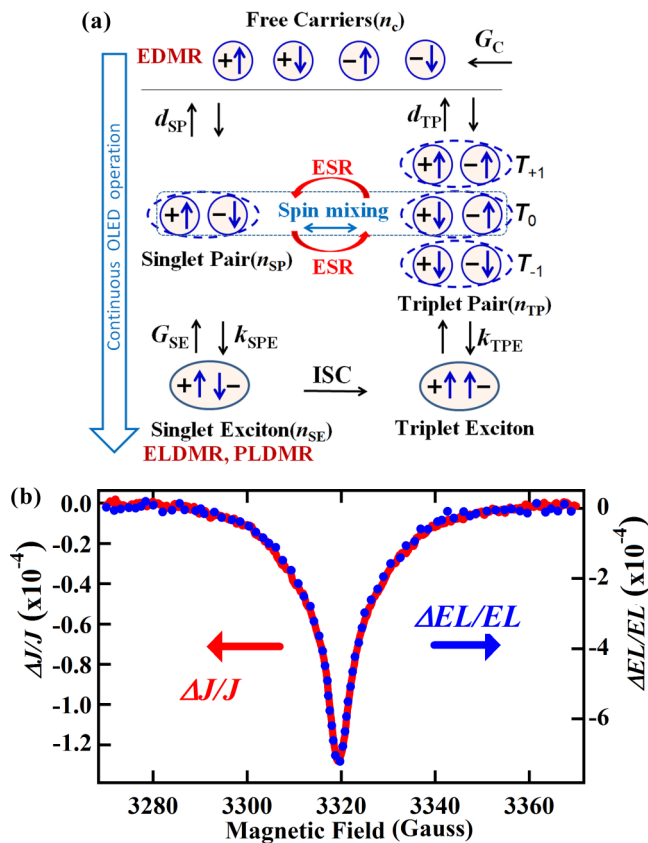


FIG. 1. (a) Illustration of model for considering EDMR and ELDMR events based on electron-hole pairs. (b) Comparison of the EDMR and ELDMR spectra measured simultaneously under 3.5-V bias.

be divided into three regions depending on the bias due to the properties of e-h pairs sensitive to the electric field. These findings provide insights into device- and magnetic properties of OLEDs.

Superyellow (SY) poly(*para*-phenylene vinylene) (PPV) purchased from Merck was used for the active layer of OLED. The OLED structure adopted was ITO/MoO₃/SY-PPV/PEI/Al where ITO is the transparent indium-tin-oxide coated glass substrate and PEI is a polyethyleneimine layer used to reduce the work function [18]. The SY-PPV layer was spin-cast from its chlorobenzene solution (5 mg/ml) on the MoO₃ layer vacuum deposited on the ITO substrate (anode). The PEI layer was spin-cast on the SY layer from the 1-propanol solution (0.5 mg/ml) and Al was vacuum deposited on the PEI layer for the cathode (30 nm). The total thickness of the PPV layer including the PEI layer was about 100 nm and the active area size of the OLED was $2 \times 3 \text{ mm}^2$. The OLED fabrication was done in a nitrogen-filled glove box and the fabricated OLED was loaded into a glass cell in the glove box and used for ESR measurements under vacuum evacuation.

All measurements were performed at room temperature. A partly modified conventional ESR spectrometer (JES-FE1XG, JEOL Ltd.) was used for all ESR measurements. Changes of current density and EL intensity induced by ESR were measured by recording the lock-in signals synchronized with the

microwave modulation (140 mW, 1.1 kHz). The EL intensity was measured with a photodiode for the EL output through an optical fiber inserted into the ESR cavity. The bias-dependent EDMR and ELDMR measurements were performed simultaneously by recording the respective lock-in signals while sweeping the bias voltage. A continuous-wave diode laser at 473 nm (640 mW/cm²) was used for photoexcitation in the PLDMR measurement. The bias dependence of the PLDMR signals was obtained by taking the difference of the ESR responses in emission intensity between signals with and without photoexcitation in order to eliminate the contribution of ELDMR. The ESR response from dark current and the off-resonance signal induced by the microwave modulation was negligibly small or eliminated.

The EDMR and ELDMR measurements were performed simultaneously for the working fluorescent OLED of SY-PPV. The EDMR and ELDMR spectra of SY-OLED under 3.5-V bias are found to resemble each other [Fig. 1(b)]. This spectral resemblance was also confirmed at other bias voltages (see Supplemental Material [19]). The EDMR and ELDMR signals are thus given by common ESR transitions regardless of the bias voltage, being consistent with the model illustrated in Fig. 1(a) assuming that the ESR transition at e-h pairs results in changing both carrier- and exciton densities. Therefore, the spin transitions at e-h pairs are responsible for both the EDMR and ELDMR signals. Indeed, the two spectra can be fitted with two Gaussian components [19], each of which may correspond to that from holes and electrons as proposed previously [20,21].

Behaviors of e-h pairs under applied electric field were examined from bias dependence of ESR signals for working OLEDs. Figures 2(a) and 2(b), respectively, show the bias dependence of the normalized EDMR and ELDMR signal intensities ($\Delta J/J$ and $\Delta I_{\text{EL}}/I_{\text{EL}}$, respectively) measured simultaneously at the resonance center (3325 G), together with the bias dependence of the current density (J) and EL intensity (I_{EL}) also measured simultaneously. Nonlinear bias-dependent relations are found both in $\Delta J/J$ and $\Delta I_{\text{EL}}/I_{\text{EL}}$, suggesting that complicated bias-dependent processes are included in the OLED operation. The observed bias-dependent EDMR and ELDMR responses may be derived from e-h pairs located at specific zones like the edge of the active layer. In order to investigate the possibility, we compared the ELDMR signals between those measured from the ITO surface and semitransparent Al surface (20 nm) using an ESR cavity with optical output ports on both sides [Fig. 2(c)]. Generally, due to the refractive index of thin active layer and the effect of cathode electrode, the output efficiency of emission from excitons varies depending on the position of exciton along the film direction [22]. Thus, if ELDMR occurs only at specific zones in the film thickness direction, the normalized ELDMR intensity should be different between the signals detected from the ITO and Al sides. In fact, their spectral shapes and $\Delta I_{\text{EL}}/I_{\text{EL}}$ values were nearly identical [Fig. 2(c)]. Furthermore, the bias dependence of $\Delta I_{\text{EL}}/I_{\text{EL}}$ at the peak position was almost the same [Fig. 2(d)]. These results demonstrate that the ELDMR response does not occur only at specific zones. Thus the observed bias-dependent ESR features represent essential EL processes occurring in common to all active EL sites.

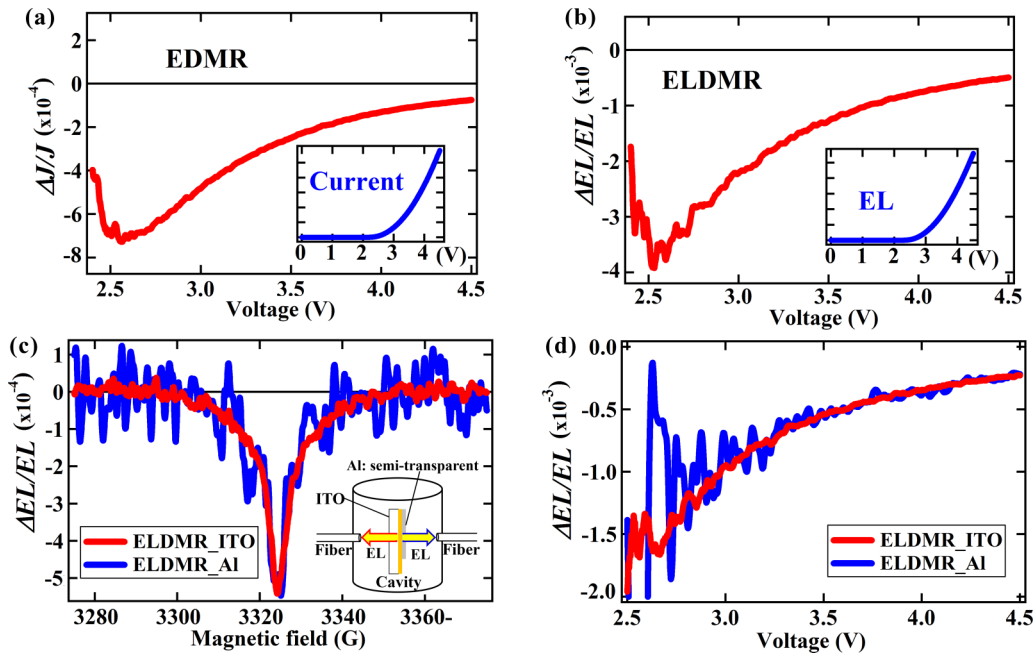


FIG. 2. Bias dependence of the normalized EDMR (a) $\Delta J/J$ and ELDMR (b) $\Delta EL/EL$ signals. The insets of (a) and (b) are the bias dependence of current and EL intensity. (c) Comparison of ELDMR spectrum between the ITO output and semitransparent Al output measured using the ESR cavity with optical output ports on both sides of the cavity (inset). (d) Comparison of the bias dependence of $\Delta EL/EL$ at the peak position obtained from the experiment in (c).

We here discuss about information obtained from bias-dependent EDMR and ELDMR signals of a working OLED. During OLED operation, carriers, e-h pairs and excitons are in equilibrium as illustrated in Fig. 1(a) [23,24]. Generally, a steady-state EL intensity I_{EL} , proportional to the density of SE(n_{SE}), is given by the following terms:

$$I_{EL} \propto n_{SE} = k_{SPE} n_{SP} \tau_{SE}, \quad (1)$$

where k_{SPE} is the transition rate of SP to SE, n_{SP} the density of SP, and τ_{SE} the lifetime of SE. For this system, the ESR transition occurring at TPs changes the equilibrium relation between SP and TP, resulting in changing n_{SP} in Eq. (1). The ELDMR intensity I_{ELDMR} and the normalized ELDMR intensity $\Delta I_{EL}/I_{EL}$ can thus be obtained as follows:

$$\Delta I_{EL} \propto \Delta n_{SE} = k_{SPE} \tau_{SE} \Delta n_{SP}, \quad (2a)$$

$$\Delta I_{EL}/I_{EL} = \Delta n_{SE}/n_{SE} = \Delta n_{SP}/n_{SP}, \quad (2b)$$

where Δ indicates a variation of each term at the ESR transition. These equations indicate that the sign of the ELDMR signal is determined by the Δn_{SP} term.

Assuming that the total current is dominated by a drift current in the bias range considered in this research, as shown by the current density $J = en_c \mu F$ where n_c is the carrier density, μ the carrier mobility, and F the strength of the internal electric field, the normalized EDMR intensity is obtained as follows:

$$\Delta J/J = \Delta n_c/n_c, \quad (3)$$

where μ and F are assumed to be independent of the ESR transition. We note that this relation is appropriate when the density of carriers injected from the electrodes linearly increases with increasing the bias, not limited to the case of

the drift current. Such a linear increase of the injected current has often been identified for the bias range above a built-in bias from spectroscopic measurements [25–27]. For Eq. (3), using the solutions of rate equations for SP and TP under or without ESR transitions, the normalized intensity is calculated as follows [19]:

$$\Delta J/J = \frac{d_{SP} k_{TPE} - d_{TP} k_{SPE}}{2G_c (d_{TP} + k_{TPE})} \Delta n_{SP}, \quad (4)$$

where d_{SP} and d_{TP} are the dissociation rates of SP and TP into carriers, respectively, k_{TPE} the transition rate of TP to TE, and G_c the injection rate of carriers from electrodes [Fig. 1(a)].

The voltage dependence of the normalized ELDMR and EDMR signals was shown to be determined by Eqs. (2b) and (4), respectively. However, since each term included in the equations could be bias dependent, the origin of the bias-dependent behaviors of the ESR signals has to be carefully considered. Particularly, carrier injection from the electrodes is expected to largely affect the voltage dependence of n_{SP} and Δn_{SP} . We here explore the use of PLDMR techniques to investigate the behavior of e-h pair purely by excluding the contribution of carrier injection from electrodes. Since exciton dissociation into e-h pairs was shown to be negligible under the bias magnitude below 5 V in the SY-OLED with the same thickness as in this study [17], e-h pairs under photoexcitation are primarily formed by couplings between photogenerated electrons and holes in the bias range. The PLDMR process thus undergoes the same path as that of ELDMR except that ELDMR includes the influence of bias-dependent carrier injection. The PLDMR intensity I_{PLDMR} is then given by the following relation:

$$\begin{aligned} I_{PLDMR} &\propto \Delta n_{SE,P} = \Delta(k_{SPE} n_{SP,P} \tau_{SE}) \\ &= k_{SPE} \tau_{SE} \Delta n_{SP,P}, \end{aligned} \quad (5)$$

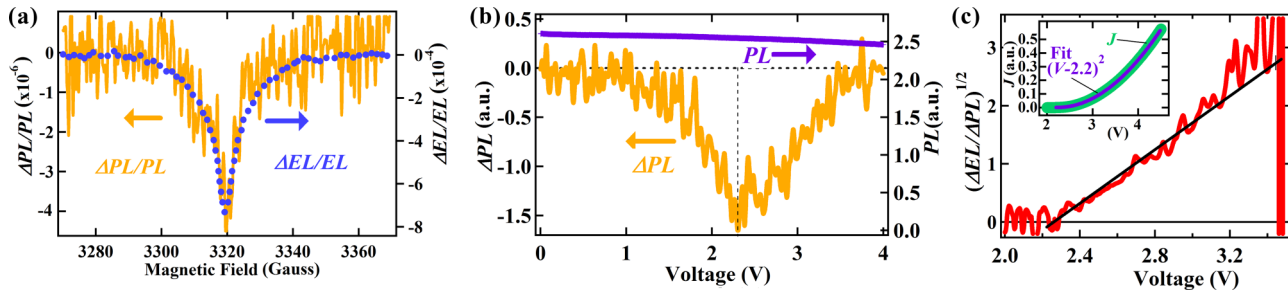


FIG. 3. (a) Comparison of the PLDMR spectrum under 2-V bias and the ELDMR spectrum obtained from the identical OLED. (b) Bias dependence of PLDMR signals measured at the resonance peak (ΔPL) and PL intensity (PL ; right axis) measured simultaneously. (c) Calculated square root of the ratio of the ELDMR intensity to the PLDMR intensity $(\Delta EL/\Delta PL)^{1/2}$ as a function of bias according to Eq. (7). The straight line is a guide for the eye. Inset of (c), fit for the current-voltage (V) characteristics of the OLED using the function of $(V - 2.2)^2$.

where $n_{SE,P}$ and $n_{SP,P}$ are the densities of photogenerated SE and SP, respectively.

We note that the PLDMR and ELDMR signals cannot be distinguished experimentally under the OLED operation. The bias dependence of PLDMR was thus derived by subtracting the contribution of ELDMR by measuring difference in the ESR response between measurements with and without photoexcitation. Comparison between the obtained PLDMR spectrum at 2 V and the ELDMR spectrum indicates that the spectra are similar to each other with the same signal sign [Fig. 3(a)], confirming that similar e-h pairs are generated under EL operation and under photoexcitation. The bias dependence of PLDMR signals measured at the resonance peak is shown in Fig. 3(b). Despite only a slight decrease found in the PL intensity with increasing bias, I_{PLDMR} decreases remarkably after a peak at 2.2 V and finally disappears: Note that the PLDMR signal cannot be detected under zero bias. The peak voltage is close to the rise point of the current at 2.0 V and nearly corresponds to the built-in voltage V_{bi} of this OLED [17]. The I_{PLDMR} -magnitude is thus determined by electric-field strength as in the previous report shown for the bias region below V_{bi} [17]. In order to confirm that the observed trend of bias-dependent PLDMR does not depend on the measurement method, double lock-in PLDMR measurements that modulate both microwave- and light intensities were also performed as a function of bias for the SY-OLED fabricated under slight exposure to the atmosphere. The exposed SY-OLED enabled use of the double lock-in technique because of its larger PLDMR signals than the present OLED fabricated without exposure to the atmosphere. The double lock-in measurements showed a similar trend in the bias-dependent PLDMR [19], indicating that the observed trend is inherent in the PLDMR signal of the OLED.

The bias-dependence curve of PLDMR intensity is probably mainly determined by the coupling strength between electron and hole in e-h pairs [17] but the curve is found to be asymmetric across the peak at 2.2 V. A gentler field dependence seen above 2.2 V suggests that injected carriers under forward bias slightly screen the electric field [28,29]. Turning to the right term of Eq. (5), when increasing the forward bias above V_{bi} , k_{SPE} is expected to be constant or increased by the electric field. Therefore, the bias-dependent reduction of PLDMR signals above V_{bi} is caused by a rapid bias-induced decrease in the $\Delta n_{\text{SP},P}$ term. This indicates that

the Δn_{SP} term of ELDMR in Eq. (2a) actually decreases with increasing a bias when removing the effect of bias on the e-h pair generation.

Since Δn_{SP} and n_{SP} are presumed to increase at the same rate with the increase of the carrier density by bias [19], $\Delta n_{\text{SE}}/n_{\text{SE}}$ is not affected by the bias-dependent carrier density according to Eq. (2b). Hence, the decrease in $\Delta n_{\text{SE}}/n_{\text{SE}}$ with increasing the bias should be attributed to a reduction in the efficiency of equilibrium shift between SP and TP after the ESR transition. Among factors affecting the equilibrium shift, the rate of ESR transition at TPs is independent of the bias. The equilibrium shift occurs primarily via the spin mixing between S and T_0 after the ESR transition and the spin mixing competes with dissociation and recombination processes of e-h pair. Therefore, the reduction in the equilibrium shift by bias is attributed to the increase of the dissociation and/or recombination rates of e-h pair competing with the spin mixing. This also provides the evidence that either or both the dissociation and recombination rates increase with increasing the bias. Such increases in the two rates reduce n_{SP} and n_{TP} . Namely, even if the generation rate of e-h pair increases by increasing the bias, the rapid increase in the dissociation/recombination rates overcomes the increase of the generation, resulting in the decrease of the pair density.

The difference in the bias-dependent intensity between the ELDMR and PLDMR signals results from the presence or absence of the contribution of carrier injection from the electrodes. Thus, reversely, comparison of their bias dependence can provide information on the bias dependence of the carrier-injection process. From Eqs. (2a) and (5), their intensity ratio is given by

$$\frac{I_{\text{ELDMR}}}{I_{\text{PLDMR}}} = \frac{\Delta n_{\text{SP}}}{\Delta n_{\text{SP},P}} = \frac{n_c^2}{n_{c,P}^2}, \quad (6)$$

where $n_{c,p}$ is the photocarrier density. Neglecting the influence of bias on $n_{c,p}$, the following relation yields the bias dependence of the carrier density injected from electrodes $n_c(V)$:

$$n_c(V) \propto (I_{\text{ELDMR}}/I_{\text{PLDMR}})^{1/2}. \quad (7)$$

The right-hand term of Eq. (7) was actually calculated below 3.5 V where the PLDMR signal was detectable, and it gave a linear relation against the bias [Fig. 3(c)]. In a simple

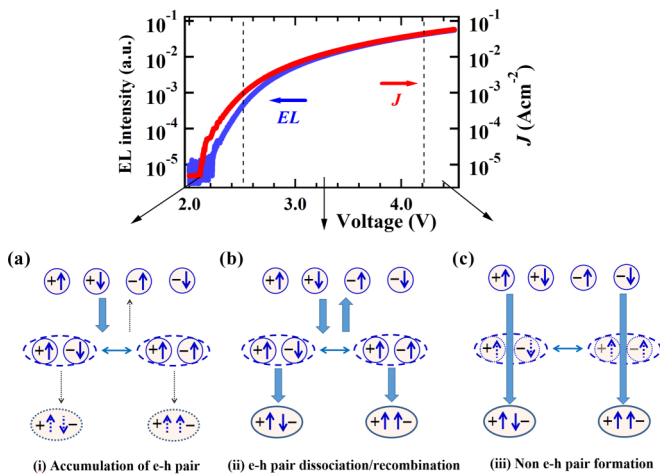


FIG. 4. Bias-dependent OLED operation predicted from ESR measurements. (a) Accumulation of electron-hole pairs. (b) Enhanced dissociation and recombination of e-h pairs. (c) Nonformation of e-h pairs.

case where the effect of trap is small, the current density in a polymer OLED has often been shown to be proportional to V^2 above V_{bi} according to a Mott-Gurney square law [30,31]. The V^2 dependence results primarily from the product of electric field and the carrier density growing both with linear V dependence. It was actually confirmed that the current-voltage characteristics of the present OLED vary according to V^2 above V_{bi} [inset of Fig. 3(c)]. The carrier density is thus expected to increase linearly above V_{bi} . Therefore the linear relation found in Fig. 3(c) is in good agreement with Eq. (7). The equation was derived by assuming that the observed ESR responses are obtained via e-h pairs. These results thus confirm that the model based on e-h pairs can correctly describe the EL operation process.

The bias-dependent behaviors of e-h pairs found here is significant in considering OLED operation. Indeed, considering the obtained ESR results, the OLED process is divided into the following three regions depending on the bias.

(i) Pair accumulation: In Figs. 2(a) and 2(b), both $\Delta I_{EL}/I_{EL}$ and $\Delta J/J$ increase from around 2.0 to 2.5 V. Their intensities are determined by the ratios of $\Delta n_{SP}/n_{SP}$ and $\Delta n_c/n_c$, respectively, and the contribution from the increase of injected carriers is canceled in the ratios. In this case, the efficiency of conversion process between SP and TP determines the bias dependence of $\Delta I_{EL}/I_{EL}$ and $\Delta J/J$ as described above. Therefore, the bias-dependent increases in $\Delta I_{EL}/I_{EL}$ and $\Delta J/J$ indicate that dissociation and recombination of e-h pairs do not proceed sufficiently against the bias-induced

increase of pairs. Namely, the e-h pairs are accumulated in this bias region [Fig. 4(a)].

(ii) Enhanced pair dissociation and recombination: Above 2.5 V, both $\Delta I_{EL}/I_{EL}$ and $\Delta J/J$ decrease with increasing the bias. As described above for ELDMR, these decreases result from a decrease in the pair density, which is caused by the increase of pair dissociation and/or recombination rates by bias. In this case, if only the dissociation is enhanced and the recombination is not enhanced by bias, the EL process will not proceed sufficiently due to enhancement only in the back reactions of e-h pair into carriers. Therefore, recombination as well as dissociation must be enhanced by bias. In fact, e-h pairs in the amorphous film have both components of taking the orientation of dissociation and recombination against the electric-field direction [17]. Importantly, the EL intensity in Fig. 2(b) increases rapidly with increasing the bias while $\Delta I_{EL}/I_{EL}$ and $\Delta J/J$ decrease. Therefore, in this bias range, both dissociation into carriers and recombination into excitons of accumulated e-h pairs progress dramatically due to the enhancement effect by electric field [Fig. 4(b)].

(iii) Negligible pair formation: Further increasing the bias, the dissociation and recombination rates of e-h pairs become larger than the generation rate of the pairs. The existence time of the e-h pair is then shortened and the effect of ESR is reduced. The extreme case of this bias region is equivalent to virtually no pair formation, meaning that electrons and holes directly form excitons after collision [Fig. 4(c)]. Such behaviors in the pair can also be found from a case where the e-h coupling strength is extremely weak. In that case, EDMR and ODMR responses, which are evidence of pair formation, may not be observed. Therefore, a system where the ESR effect is absent probably means that the e-h coupling of the system is extremely weak.

In summary, the bias-dependent behaviors of e-h pair under OLED operation were investigated via combining EDMR, ELDMR, and PLDMR techniques, and the following conclusions were obtained. We showed evidence that e-h pairs are generated with completely different bias dependence from carriers and excitons. This feature results from the field-sensitive properties of e-h pairs. The model assuming e-h pairs as an intermediate state was shown to describe well the observed EL features. The EL operation is divided into three regions depending on the bias: i) pair-accumulation, ii) pair-dissociation/recombination and iii) non-pair-formation regions.

This work was supported in part by JSPS KAKENHI Grant No. 17H03135 and by the OCU Strategic Research Grant 2017 for basic researches.

[1] C. W. Tang and S. A. Vanslyke, *Appl. Phys. Lett.* **51**, 913 (1987).
 [2] J. H. Burroughes, D. D. C. Bradley, A. R. Brown, R. N. Marks, K. Mackay, R. H. Friend, P. L. Burn, and A. B. Holmes, *Nature (London)* **347**, 539 (1990).
 [3] M. A. Baldo, D. F. O'Brien, Y. You, A. Shoustikov, S. Sibley, M. E. Thompson, and S. R. Forrest, *Nature (London)* **395**, 151 (1998).

[4] M. A. Baldo, S. Lamansky, P. E. Burrows, M. E. Thompson, and S. R. Forrest, *Appl. Phys. Lett.* **75**, 4 (1999).
 [5] J. Lee, H. F. Chen, T. Batagoda, C. Coburn, P. I. Djurovich, M. E. Thompson, and S. R. Forrest, *Nat. Mater.* **15**, 92 (2016).
 [6] H. Uoyama, K. Goushi, K. Shizu, H. Nomura, and C. Adachi, *Nature (London)* **492**, 234 (2012).
 [7] H. Kaji *et al.*, *Nat. Commun.* **6**, 8476 (2015).

- [8] Z. Y. Yang, Z. Mao, Z. L. Xie, Y. Zhang, S. W. Liu, J. Zhao, J. R. Xu, Z. G. Chi, and M. P. Aldred, *Chem. Soc. Rev.* **46**, 915 (2017).
- [9] B. Hu and Y. Wu, *Nat. Mater.* **6**, 985 (2007).
- [10] F. J. Wang, H. Bässler, and Z. V. Vardeny, *Phys. Rev. Lett.* **101**, 236805 (2008).
- [11] U. Niedermeier, M. Vieth, R. Patzold, W. Sarfert, and H. von Seggern, *Appl. Phys. Lett.* **92**, 193309 (2008).
- [12] T. D. Nguyen, G. Hukic-Markosian, F. J. Wang, L. Wojcik, X. G. Li, E. Ehrenfreund, and Z. V. Vardeny, *Nat. Mater.* **9**, 345 (2010).
- [13] T. D. Nguyen, B. R. Gautam, E. Ehrenfreund, and Z. V. Vardeny, *Phys. Rev. Lett.* **105**, 166804 (2010).
- [14] F. Macia, F. J. Wang, N. J. Harmon, A. D. Kent, M. Wohlgenannt, and M. E. Flatte, *Nat. Commun.* **5**, 3609 (2014).
- [15] Y. C. Hsiao, T. Wu, M. X. Li, and B. Hu, *Adv. Mater.* **27**, 2899 (2015).
- [16] Y. F. Wang, K. Sahin-Tiras, N. J. Harmon, M. Wohlgenannt, and M. E. Flatte, *Phys. Rev. X* **6**, 011011 (2016).
- [17] K. Kanemoto, S. Hatanaka, K. Kimura, Y. Ueda, and H. Matsuoka, *Phys. Rev. Mater.* **1**, 022601 (R) (2017).
- [18] Y. H. Zhou *et al.*, *Science* **336**, 327 (2012).
- [19] See Supplemental Material at <http://link.aps.org/supplemental/10.1103/PhysRevMaterials.2.115201> for detailed comparison of EDMR and ELDMR spectra, the spectral fits for EDMR spectra, theoretical background for the EDMR and ELDMR signals and the PLDMR result by a double modulation technique.
- [20] D. R. McCamey, K. J. van Schooten, W. J. Baker, S. Y. Lee, S. Y. Paik, J. M. Lupton, and C. Boehme, *Phys. Rev. Lett.* **104**, 017601 (2010).
- [21] S. Y. Lee, S. Y. Paik, D. R. McCamey, J. Yu, P. L. Burn, J. M. Lupton, and C. Boehme, *J. Am. Chem. Soc.* **133**, 2019 (2011).
- [22] L. H. Smith, J. A. E. Wasey, and W. L. Barnes, *Appl. Phys. Lett.* **84**, 2986 (2004).
- [23] D. R. McCamey, H. A. Seipel, S. Y. Paik, M. J. Walter, N. J. Borys, J. M. Lupton, and C. Boehme, *Nat. Mater.* **7**, 723 (2008).
- [24] S.-Y. Lee, S. Paik, D. R. McCamey, and C. Boehme, *Phys. Rev. B* **86**, 115204 (2012).
- [25] A. S. Dhoot, D. S. Ginger, D. Beljonne, Z. Shuai, and N. C. Greenham, *Chem. Phys. Lett.* **360**, 195 (2002).
- [26] K. Kanemoto, M. Yasui, T. Higuchi, D. Kosumi, I. Akai, T. Karasawa, and H. Hashimoto, *Phys. Rev. B* **83**, 205203 (2011).
- [27] K. Kanemoto, M. Yasui, D. Kosumi, A. Ogata, M. Sugisaki, T. Karasawa, I. Akai, and H. Hashimoto, *Phys. Rev. Lett.* **103**, 187402 (2009).
- [28] P. J. Brewer, P. A. Lane, A. J. deMello, D. D. C. Bradley, and J. C. deMello, *Adv. Funct. Mater.* **14**, 562 (2004).
- [29] K. Kanemoto, T. Takahashi, and H. Hashimoto, *Appl. Phys. Lett.* **109**, 013301 (2016).
- [30] M. A. Lampert and P. Mark, *Current Injection in Solids* (Academic, New York, 1970).
- [31] H. C. F. Martens, W. F. Pasveer, H. B. Brom, J. N. Huiberts, and P. W. M. Blom, *Phys. Rev. B* **63**, 125328 (2001).